Astronomy & Astrophysics manuscript no. main
August 6, 2022

Letter to the Editor

Mass limits for stationary protoplanetary accretion disks

F. Ragossnig[1], L. Gehrig[1], E. A. Dorfi[1], D. Steiner[1], and A. Stökl[1]

Institute for Astrophysics (IfA), University of Vienna, Türkenschanzstrasse 17, A-1180 Vienna
e-mail: florian.ragossnig@univie.ac.at

Received September 15, 1996; accepted March 16, 1997

ABSTRACT

Context. The collapse of interstellar gaseous clouds towards a protostar leads to the formation of accretion disks around the central star. Such disks can be dynamically stable if they settle in an axisymmetric state.
Aims. In this letter, we investigate the long-term stability of astrophysical viscous disks around various protostars.
Methods. We apply an implicit numerical code which solves the equations of radiation hydrodynamics and treats turbulence-induced viscosity according to the α-viscosity model.
Results. We show how the viscosity is related to the disk mass. A stability criterion to determine the maximum disk mass can be formulated. We analyse such instabilities for a variety of radial points with different orbital distances from the host star and discuss the feedback on the disk in the event of an unstable protoplanetary disk. Additionally, we examine the critical disk-mass for disks with variable outer boundaries and compare them to observations of protostellar disks in the Upper Scorpius OB Association and near the Lupus complex. We derive an easily applicable method to obtain an estimate for maximum disk masses when the outer disk radius ins known.

Key words. Accretion, accretion disks – Methods: numerical – Protoplanetary disks – Radiation: dynamics

1. Introduction

A possible solution to the angular momentum problem during the collapse of a gaseous cloud towards a protostar is the formation of an accretion disk, where diffuse matter (gas and dust) orbits around and gets accreted onto a central source (eg. Mestel 1965). Since the total angular momentum of the disk has to be conserved, angular momentum must be transported outwards while mass is moving inwards to the centre of the disk. According to the Rayleigh stability criterion

$$\frac{\partial\left(r^2\Omega\right)}{\partial r} > 0\,, \tag{1}$$

where r is the orbital distance of a mass element and Ω it's angular velocity, mass accretion is expected to be a laminar flow and thus prevents a pure hydrodynamic mechanism to be responsible for the angular momentum transport (e.g. Lynden-Bell & Pringle 1974). Although the accretion flow is caused by viscous forces, the source of such a turbulence-induced viscosity is still under debate (e.g. Bai & Stone 2013). Up to now, the most accepted model is the α-viscosity model, which assumes subsonic turbulences, where the eddies are limited by the scale height H_P of the disk (Shakura & Sunyaev 1973). Hence, the kinematic viscosity ν can be written as

$$\nu = \alpha c_\mathrm{S} H_\mathrm{P}\,, \tag{2}$$

where α is a constant viscosity parameter, c_S is the speed of sound and H_P is the scale height of the disk.

Recent ALMA (Atacama Large Millimetre Array) data shows that 75% of the observed disks around T-Tauri stars are axially symmetric (Andrews et al. 2018). Since a protoplanetary disk can only be axially symmetric if the disk is dynamically stable, these data suggest that most protoplanetary disks must be stationary, at least for a considerable amount of time. This assumption is supported by recent protoplanetary disk simulations, where the disk remains in an axisymmetric state for ~80% of the lifetime of the disk (Vorobyov et al. 2019). A stability criterion for astrophysical viscous disks has first been presented by Pringle (1981), where a disturbance μ' of the dynamic viscosity $\mu = \nu\Sigma$ obeys the following equation

$$\partial_t(\mu') = \frac{\partial\mu}{\partial\Sigma}\,\frac{3}{r}\left[r^{1/2}\partial_r\left(\mu r^{1/2}\right)\right]\,. \tag{3}$$

This diffusion equation tends to become unstable if

$$\frac{\partial\mu}{\partial\Sigma} < 0\,. \tag{4}$$

Here, Σ is the surface density of the disk. Since Eq. 4 is directly related to the disk-mass, we suggest that there is an upper mass limit for a dynamically stable protoplanetary disk.

To test this assumption, long term global evolution simulations of protoplanetary disks are necessary. For a simple description, we can assume a disk with negligible mass around a star with mass M_* in centrifugal balance. Thus, for a radial distance r we obtain an orbital velocity which is proportional to $r^{-1/2}$. According to Kepler's 3$^{\mathrm{rd}}$ law, this implies that when scaling the radius by a factor of 100, the orbital periods vary by a factor of 1000. This physical requirement immediately hinders all explicit numerical simulations as a consequence of the Curant-Friedrichs-Levy (CFL) condition (Courant et al. 1928), which limits the timestep to a fraction of the orbital period at the inner boundary of the disk. Since the requirement of a dynamically stable viscous disk is axis-symmetry, we can adopt an implicit scheme to overcome the timestep restrictions due to the CFL-condition. For our stability studies, we utilized the TAPIR code (The Adaptive Implicit RHD) for axisymmetric disks (Ragossnig et al. 2019).

2. Model Description

The TAPIR code is an implicit 1+1D code which assumes axial-symmetry and solves the equations of radiation hydrodynamics (RHD) in the radial direction. The equations are discretized in conservation form on a radial adaptive grid, the advection is done by a 2nd-order scheme. Further details on the numerical method are described in Ragossnig et al. (2019). The vertical disk structure is defined via a local hydrostatic equilibrium and thus the physical quantities can be obtained via integration in z-direction using the equation of state (EOS). Additionally, a consistent formulation of the self-gravity of the disk is included.

2.1. Initial model and boundary conditions

Since implicit schemes require the presence of an initial model which represents a full RHD-solution of the problem (e.g. Dorfi 1998), we start with a disk with a uniform density distribution (similar to Bath & Pringle 1981). The stellar parameters, such as the luminosity L_* and the radius R_*, for the central star with mass M_* are taken from Palla & Stahler (1991) and Fletcher & Stahler (1994) respectively.

The exact position of the inner and outer boundary of the disk is hard to define since the inner boundary depends on the rotational speed and the magnetic field of the star. The outer boundary is basically defined at the location of the interstellar medium (ISM) and thus determines the mass of the disk (see Sect. 3). The position of the inner disk boundary is still under investigation (Ragossnig et al. 2019) and depends on the physical properties of the star and the accretion rate of the disk (Hartmann et al. 2016). We set the inner boundary to the corotation radius $r_{\rm co}$. As $r_{\rm co}$ defines the position where the rotational speed of the star matches the angular velocity of the disk, mass will accrete onto the star in a free-fall and thus represents a physical boundary for the disk. Since the corotation radius itself depends on the star's rotational period Ω_* and for T-Tauri stars Ω_* is approximately 2 days (Herbst et al. 2001), we can formulate the stellar rotational period as a fraction of the Keplerian orbital period on the stellar surface $\Omega_{\rm K,*}$

$$\Omega_* = \beta \Omega_{\rm K,*} \,, \tag{5}$$

where $\beta \sim 0.1$ is an average value for stars with masses between $0.1 < M_\odot < 2$. Setting the Kepler period at the corotation radius $\Omega_{\rm K,co} = \beta \Omega_{\rm K,*}$ leads to an estimate of $r_{\rm co}$

$$r_{\rm co} = \left(\frac{G M_*}{(\beta \Omega_{\rm K,*})^2} \right)^{1/3} . \tag{6}$$

To ensure that the implicit scheme converges towards the final physical solution, an initial model is required which is a full solution of the RHD equations. Since our initial model is entirely arbitrary, we need to step-wise adjust the model. Therefore, we first assume no fluid flow through the disk and let the initial model adjust thermally to the stellar environment. Once the thermal profile has been established, we define pressureless inflow and outflow conditions at the inner and outer disk boundary. The disk can now evolve thermally and dynamically to the final solution. A surface density profile for a stable protoplanetary disk around a star with $M_* = 1.0\,{\rm M}_\odot$, with the inner boundary at $r_{\rm in} = r_{\rm co} = 0.091$ AU and the outer boundary at $r_{\rm out} = 1$ AU, is presented in Fig. 1.

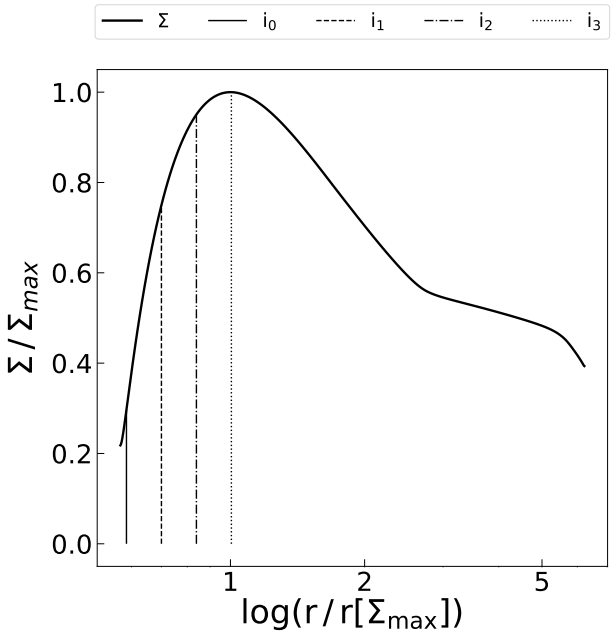

Fig. 1. Surface density profile of a stable protoplanetary disk around a star with $M_* = 1.0\,{\rm M}_\odot$, with a distance from the host star of $r_{\rm in} = 0.091$ AU and an outer radius of $r_{\rm out} = 1$ AU. The surface density Σ is given in values of its maximum $\Sigma_{\rm max}$, the radius r is given in values of the radius at the density maximum $r(\Sigma{\rm max})$ and plotted logarithmically. The different vertical lines represent radial test points which are tested for stability.

2.2. Stability

From Eq. 4 we see that the stability equation is a local stability criterion. However a large number of numerical computations show that it also globally valid. Since the viscosity is most effective close to the star (in the area in front of the surface density maximum; see Fig. 1), we found that we only need to test at radial points within this viscous less effective region.

In Fig. 1 we see the different radial points i_0 (dotted), i_1 (dashed-dotted), i_2 (dashed) and i_3 (solid). The radial point i_3 sits on the position of the surface density maximum and the other points, i_0 to i_2, are distributed logarithmically equidistant to the left. In the following figures the linestyles match the location of these radial points.

3. Results

To test the existence of a critical mass according to the stability criterion Eq. 4, we investigate the long term evolution of a dynamically stable disk (see Sec. 2.1) at 4 different radial points in the viscous most effective region (Sec. 2.2). In Fig. 2 we visualize the stability criterion via the dynamic viscosity μ as a function of the surface density Σ in normalised units. The left panel shows a stable disk with a disk mass of $m_{\rm D} = 1.2\%\ M_*$ and the middle panel an unstable disk with $m_{\rm D} = 3.5\%\ M_*$, around a star with mass $M_* = 1\,{\rm M}_\odot$, radius $r_* = 4.88\,{\rm R}_\odot$ and luminosity $L_* = 6.887\,{\rm L}_\odot$ (compare Palla & Stahler 1991). For both disks we set the inner boundary to $r_{\rm in} = 0.050$ AU (according to Eq. 6) and the outer boundary to $r_{\rm out} = 10$ AU. One can see that for the stable disk (left panel), the viscosity gradient at a test point (i_0 to i_3) remains positive throughout the entire simulation time ($t_{\rm sim} = 10^{10}$ yrs), whereas in the unstable case (middle panel), the

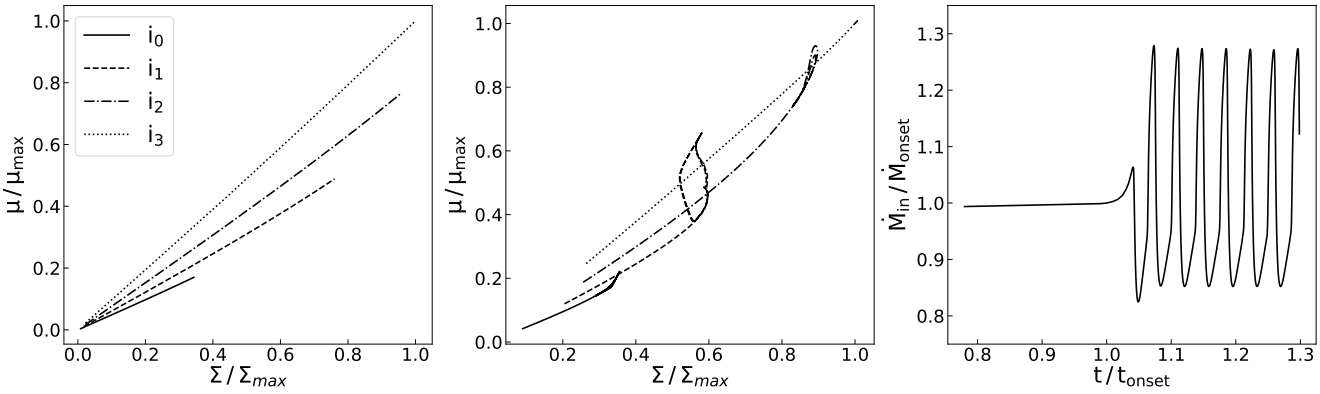

Fig. 2. Visualisation of a stable (left panel) and an unstable protoplanetary disk (middle panel). Here the dynamic viscosity μ is plotted as a function of the surface density and both values are presented in dimensionless variables. The individual lines i_0 to i_3 represent the long term stability ($\tau = 10^{10}$ yrs) of radial test points. In the stable case (left) the viscosity gradient (see Eq. 4) remains positive for the entire simulation time whereas in the unstable case (middle) the gradient shifts to negative values and results in feedback loops. These loops manifest in an oscillating accretion flow (right panel) over the inner boundary which contradicts the matter that the mass-flux has the be constant throughout the entire radial extension for dynamically stable disks. The right panel shows the oscillating accretion flow $\dot{M}$ in values of the critical mass-flux $\dot{M}_{\rm crit}$ over the inner boundary in case of instability as a function of time in values of the instability onset time $t_{\rm onset}$.

gradient, at some time, switches its sign. Although $\partial\mu/\partial\Sigma < 0$ appears at all test points, some of the points are showing more pronounced loop features due to a locally more efficient viscosity. The change to a negative viscosity gradient for a radial point results in an oscillating mass-flux over the inner boundary. In Fig. 2, right panel, we show the mass-flux over the inner boundary $\dot{M}_{\rm in}$ as a function of time, normalised to the values at the onset of the instability in the case of an unstable disk (middle panel). The oscillation of $\dot{M}_{\rm in}$ clearly contradicts with the stability requirement of a constant mass-flux throughout the entire disk.

Since $\partial\mu/\partial\Sigma = 0$ represents the upper mass limit for dynamically stable viscous disks, we tested different sized disks around various stars to the maximum mass they can contain, according to the stability criterion. Additionally, we compare our results to recent high resolution surveys of mostly axisymmetric disks near the Lupus complex (Ansdell et al. 2016) and disks in the Upper Scorpius OB Association (Barenfeld et al. 2016). In Fig. 3 we show the calculated critical mass in stellar masses as a function of the outer boundary $r_{\rm out}$ for a star with $M_* = 0.4\,{\rm M}_\odot$ (dots). These data points represent disks around a star with an averaged stellar mass of the observational data and outer disk-radii at 1, 5, 10, 15, 30, 50 and 100 AU. The other data points denote the observed disk-mass (dust and gas) in either the Lupus survey (triangles) or the Scorpio OB Association (x-marker). One can see that all observed disk masses are clearly below the critical mass and thus support the validity of our estimate.

Moreover, we find that the critical mass for disks with different radii around the same host star are connected via two power law fits. For massive disks, the disk-gas becomes gravitationally unstable if the Toomre criterion is fulfilled (Armitage 2013)

$$Q = \frac{c_{\rm S}\Omega_{\rm K}}{\pi G\Sigma} > 1\ . \tag{7}$$

This parameter determines the maximum mass for axisymmetric configurations. Nevertheless, if the disk mass reaches a certain lower limit, the viscous stability criterion Eq. 4 becomes dominant. The transition of the two stability regimes is plotted as a dotted vertical line in Fig. 3 ($R_{\rm SW}$). We find that our model predicts the exponents for the fit functions to be $\xi_\nu = 1.3$ and $\xi_{\rm T} = 0.5$ for the viscous and Toomre stable case respectively. Assuming that for a dynamically stable disk $c_{\rm S}^2 \propto T \propto r^{-3/4}$, where $c_{\rm S}$ is the speed of sound, T the disk gas temperature and r the radial distance from the host star, one can see that the disk-mass $m_{\rm D}$ is related to the mass-flux $\dot{M}$ according to (see Armitage 2013, page 68-87)

$$m_{\rm D} \propto \dot{M} r^{\frac{5}{4}}\ . \tag{8}$$

Since Eq. 8 is valid only in the viscous stable case and considering that our model solves a coupled set of partial differential equations and that we set the inner boundary to the corotation radius (which depends on the different stellar parameters), our computations are in excellent agreement with the simple estimate for the exponent ($\xi = 5/4$; Eq. 8).

In the gravitationally unstable case, our model predicts a fit parameter of $\xi_{\rm T} = 0.5$ which is exact the value of recent findings by Haworth et al. (2020), where the authors studied the stability of massive disks around low-mass stars.

Hence, a basic estimate for the critical disk mass $m_{\rm D,max}$ as a function of the outer disk radius can be derived by combining the two fit functions in the viscous stable and gravitationally stable case respectively

$$m_{\rm D,max} \approx \begin{cases} r_{\rm out}^{\xi_\nu}, & \text{for } r_{\rm out} < R_{\rm SW} \\ r_{\rm out}^{\xi_{\rm T}}, & \text{for } r_{\rm out} \geq R_{\rm SW} \end{cases}\ , \tag{9}$$

where $r_{\rm out}$ is the outer disk radius, α_ν and $\alpha_{\rm T}$ the fit parameter for the viscous case and the Toomre case respectively and $R_{\rm SW} = 15$ AU the position of the transition from viscous to gravitational instability.

4. Conclusion

In this letter, we apply an implicit numerical model which solves the axially-symmetric, time-dependent equations of radiation hydrodynamics, for estimating the upper mass limit for dynamically stable astrophysical viscous disks. Although applying axial symmetry restricts the problem to one dimension, such implicit

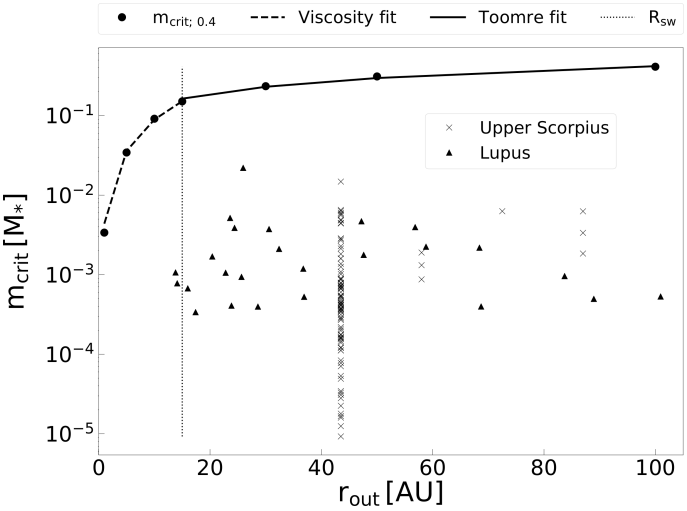

Fig. 3. Critical disk mass $m_{\rm crit}$ in stellar masses as a function of the outer disk radius $r_{\rm out}$. The dotted datapoints are our model results for disks around a stellar mass with $M_* = 0.4\,{\rm M}_\odot$, which represents the averaged stellar mass for the observed disks in the Lupus survey (triangles) and Scorpius OB Association (x-markers). The dashed line is the power law fit for viscous stable disks, the solid line the power law fit for gravitationally stable disks. Since the survey data mainly contains axisymmetric disks, our model can clearly predict an upper mass limit for protostellar disks.

computations allow an accurate description of the disk structure over time-scales much longer than several orbital periods. We emphasize that protoplanetary disks can only be dynamically stable if they persist in an axisymmetric configuration and thus justify a one-dimensional approach. Furthermore, this assumption is supported by recent observations (Andrews et al. 2018) and simulation data (Vorobyov et al. 2019) which indicate that protoplanetary disks spend approximately 80% of their lifetime in an axisymmetric state.

We show that varying the disk mass either via the initial model (Fig. 2) or the outer radius (Fig. 3) can lead to an instability if the stability criterion (Eq. 4), which was first proposed by Pringle (1981), is not fulfilled. Since such an instability manifests in an oscillating mass-flux over the inner boundary but dynamical stability requires a constant mass-flux throughout the entire disk, an axisymmetric disk structure can no longer be obtained.

The onset of this instability is independent of the thermodynamical properties of the gas. Protoplanetary disks become unable to handle stationary accretion rates up to a certain limit which now can be computed by our numerical method.

Moreover, the stability criterion Eq. 4 implies a maximum mass which can be contained in a disk which remains dynamically stable. We provide a relation to estimate the critical mass for a protoplanetary disk if the outer disk radius is known (Eq. 9). We point out that value for the exponent in this mass-radius relation depends on the stellar mass and thus conducting more simulations with different stellar masses will lead to better estimates. Further computations with a non-constant viscosity, simulating layered disks will be subject to further investigations and thus presented in follow-up publications.

Acknowledgements. The authors acknowledge support by the FWF NFN project S116 “Pathways to Habitability: From Disks to Active Stars, Planets and Life”, the related subprojects S11601-N16 “Hydrodynamics and Radiation in Young Star Disk Systems” and S11604-N16 “Radiation & Wind Evolution from T Tauri Phase to ZAMS and Beyond”. This publication is supported by the Austrian Science Fund (FWF).

References

Andrews, S. M., Huang, J., Pérez, L. M., et al. 2018
Ansdell, M., Williams, J. P., van der Marel, N., et al. 2016, ApJ, 828, 46
Armitage, P. J. 2013, Astrophysics of Planet Formation
Bai, X.-N. & Stone, J. M. 2013, ApJ, 769, 76
Barenfeld, S. A., Carpenter, J. M., Ricci, L., & Isella, A. 2016, ApJ, 827, 142
Bath, G. T. & Pringle, J. E. 1981, MNRAS, 194, 967
Courant, R., Friedrichs, K., & Lewy, H. 1928, Mathematische Annalen, 100, 32
Dorfi, E. 1998, Saas-Fee Advanced Courses, Vol. 27, Computational Methods for Astrophysical Fluid Flow, ed. O. Steiner & A. Gautschy (Berlin/Heidelberg: Springer-Verlag), 263–341
Fletcher, A. B. & Stahler, S. W. 1994, ApJ, 435, 313
Hartmann, L., Herczeg, G., & Calvet, N. 2016, ARA&A, 54, 135
Haworth, T. J., Cadman, J., Meru, F., et al. 2020, arXiv e-prints, arXiv:2001.06225
Herbst, W., Bailer-Jones, C. A. L., & Mundt, R. 2001, ApJ, 554, L197
Lynden-Bell, D. & Pringle, J. E. 1974, MNRAS, 168, 603
Mestel, L. 1965, Quarterly Journal of the Royal Astronomical Society, 6, 161
Palla, F. & Stahler, S. W. 1991, ApJ, 375, 288
Pringle, J. E. 1981, ARA&A, 19, 137
Ragossnig, F., Dorfi, E. A., Ratschiner, B., et al. 2019
Shakura, N. I. & Sunyaev, R. A. 1973, A&A, 24, 337
Vorobyov, E. I., Skliarevskii, A. M., Elbakyan, V. G., et al. 2019, arXiv e-prints, arXiv:1905.11335